

LASER PROTON ACCELERATOR WITH IMPROVED REPEATABILITY AT PEKING UNIVERSITY*

Y. Shou, Y. Geng, C. Li, R. Li, Q. Liao, C. Lin, H. Lu, W. Ma, P. Wang, M. Wu, X. Xu, X. Yan[†], Y. Zhao, J. Zhu, State Key Laboratory of Nuclear Physics and Technology, Beijing, China

Abstract

The repeatability of laser proton accelerator is mainly limited by laser plasma interaction, laser target coupling and laser parameter variation. In our recent experiments performed on the Compact Laser Plasma Accelerator at Peking University, gain of proton beams with improved repeatability is demonstrated. In order to control the laser plasma interaction in pre-plasma, cross polarized-wave generation technique is employed to provide a laser pulse with an ultrahigh contrast of 10^{-10} . A semi-automatic laser and target alignment system with a sensitivity of few microns is employed. The repetition rate of the laser proton accelerator is at the level of 0.1 Hz which is beneficial to decrease laser parameter variation. The shot-to-shot variation of proton energies is about 9% for a level of confidence of 0.95.

INTRODUCTION

Thanks to the development of laser technologies, laser plasma accelerators have made great progress since first proposed in 1979 [1]. Several main laser proton acceleration mechanisms have been studied theoretically and experimentally, such as target normal sheath acceleration (TNSA) [2-4], radiation pressure acceleration (RPA) [5-7], collisionless shock acceleration (CSA) [8, 9] and break-out afterburner acceleration (BOA) [10]. Generation of 93 MeV proton beams using femtosecond laser pulse has been reported in 2016 [7].

Laser proton accelerators are attractive for building compact particle accelerators, since they have three orders higher acceleration gradient compared to conventional accelerators. Proton beams gained from laser proton accelerators have the advantages of short duration, small emittance and extreme brightness, which make them suitable for wide potential applications including cancer therapy [11], proton imaging [12], nuclear reactions [13] and injectors for conventional accelerators [14]. However, current laser-driven proton beams show wide energy spread and poor repeatability, which limit those application [15]. Great efforts have been made in improving the repeatability of laser proton accelerators [16-18]. Recently Y. Gao et al. have demonstrated experiments with 0.5 Hz repetition rate and realized shot-to-shot variation of about 27% for a level of confidence of 0.95 [19].

The shot-to-shot variations of laser-driven proton beams are mainly due to instabilities in laser plasma interaction, inaccuracies from laser target coupling and fluctuations of laser parameters. In our recent experiments performed on the Compact Laser Plasma Accelerator (CLAPA) at Peking University [20, 21], gain of proton beams with improved repeatability is demonstrated. Fig-

ure 1 shows the layout of our laser proton acceleration system. With the help of cross polarized-wave (XPW) system for pulse cleaning, the laser pulse's nanosecond contrast is at the level of 10^{-10} . A semi-automatic target alignment system with a sensitivity of 5 μm is employed to ensure the laser target coupling accuracy. Recently, the shot-to-shot variation of the cut-off proton energies has been reduced to about 9% for a level of confidence of 0.95.

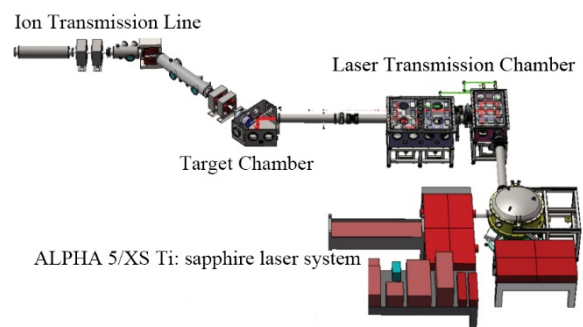


Figure 1: Layout of the CLAPA laser proton acceleration system.

CLAPA LASER SYSTEM

The CLAPA laser system is based on Ti: Sapphire with double CPA structure. The laser pulse has a central wavelength of 800 nm and a bandwidth of 45 nm. KHz pulses are generated through the first stage of CPA from an 82 MHz oscillator. In order to enhance the laser temporal contrast, XPW system for pulse cleaning is employed before the second CPA stage. A pulse with total energy of 7 J can be achieved in the output of the last amplifier, which is then sent into a vacuum compressor. A deformable mirror is mounted before the compressor to correct wavefront aberrations. Finally, a 5 J laser pulse with full width at half maximum (FWHM) pulse duration of 25 fs can be achieved. Measurements using free space InGaAs detector with a high speed oscilloscope show that the laser pulse's nanosecond contrast is at the level of 10^{-10} . Picosecond time scale contrast was measured using a third order scanning autocorrelator. The results show that the laser contrast is 10^{-10} at 40 ps before the main pulse and prepulses appear at -38 ps as well as -19 ps with contrast 10^{-9} . The shot-to-shot fluctuations of laser pulse energy are less than 2% in our 5 Hz repetition frequency tests.

* Work supported by National Basic Research Program of China (Grant No. 2013CBA01502), National Natural Science Foundation of China (Grants No. 11575011) and National Grand Instrument Project (2012YQ030142).

[†] x.yan@pku.edu.cn

TARGET ALIGNMENT SYSTEM

Several alignment techniques, for instance, microscope system [18], transverse optical shadowgraphy [22] and retro-focusing technique [23] have been proposed for precise laser target coupling. In our experiment, we employ a target alignment system consisting of two main components: one target part and one microscope part. The target part is a special-designed target wheel controlled by five-axis motorized stages. Figure 2 displays the schematic of the microscope system controlled by three-axis motorized linear stages. A 50-fold long working distance microscopic objective is employed to acquire magnifying images of the target rear surface. Two different magnifications 10-fold (CCD1) and 50-fold (CCD2) can be achieved simultaneously with the help of a beam splitter. The 10-fold camera has the advantage of larger field of view, which is beneficial for seeking the laser spot. At the same time, the 50-fold camera is employed for laser spot optimization and high precision laser target coupling.

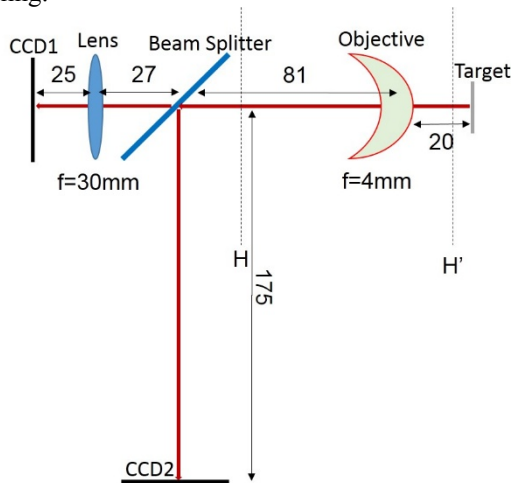


Figure 2: Schematic of the microscope system. The omitted unit is millimetre. Two different magnifications 10-fold (CCD1) and 50-fold (CCD2) can be achieved simultaneously with the help of a beam splitter.

Real picture of the target alignment system is shown in Fig. 3. Laser target coupling is realized by three steps. Firstly, the microscope system should be moved to a reference position based on the Thomson parabola spectrometer. Secondly, we move every target to the focal plane of the objective. Images of the target rear surface with different target thicknesses and materials are shown in Fig. 4. Thirdly, the off axis parabolic (OAP) mirror is optimized to position the laser waist on the focal plane.

The target alignment system is hidden in a safe place during shots. We have improved the repetition rate by recording the coordinates of all targets ahead of the first shot. What we should do before a shot is just moving the target wheel. However, a two-stage laser shutter system is employed for the sake of safety, which limits the further improvement of repetition rate. New shutter system is in development to resolve this problem.



Figure 3: Real picture of the target alignment system.

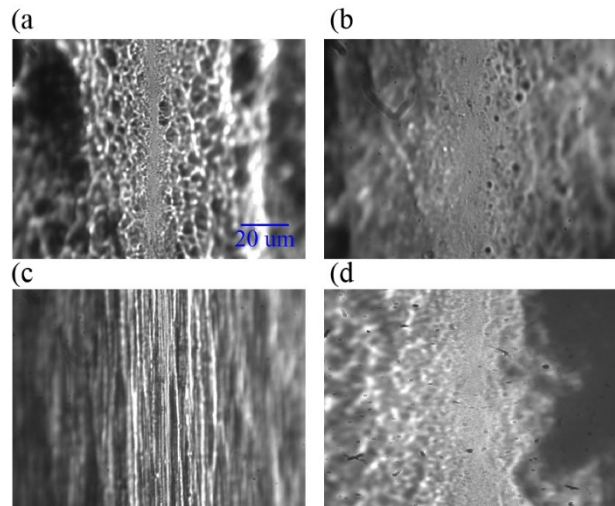


Figure 4: Images of the target rear surface. (a). 1.2 μm thick aluminium target, (b). 2.5 μm thick aluminium target, (c). 3 μm thick titanium target, (d). 50 nm thick diamond-like carbon target, respectively. The scales of the figures are the same.

The main source of uncertainty between target and laser waist is due to the objective's depth of focus and the laser's angle of incidence. The precision of the target alignment system is within 5 μm .

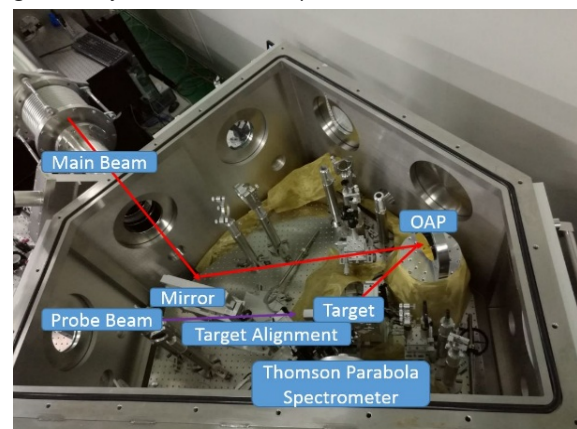


Figure 5: Target chamber for laser proton acceleration.

EXPERIMENT RESULTS

Preliminary experiment has been performed to study the repeatability of laser-driven proton beams. The experimental arrangement is shown in the Fig. 5. A p-polarized, 25 fs and energy of nearly 0.8 J laser pulse was focused using an $f/3.5$ OAP on a 0.8 μm thick aluminium target at an angle of 45° . The repetition period is 30 seconds per shot.

The results of 17 continuous shots are displayed in Fig. 6. Proton beams with average cut-off energy of 4.5 MeV and shot-to-shot variation of about 9% have been demonstrated.

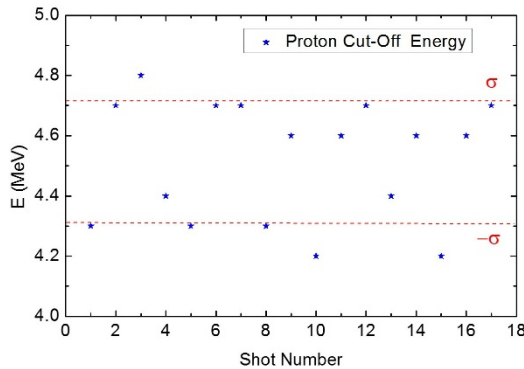


Figure 6: The shot-to-shot results of proton cut-off energy.

CONCLUSION

In conclusion, we have performed experiments with improved repeatability on the laser proton accelerator at Peking University. Thanks to the ultrahigh laser contrast, the accurate target alignment system and the high repetition rate, 9% shot-to-shot variation of proton energies has been successfully demonstrated.

ACKNOWLEDGEMENT

The CLAPA has been designed and built with the effort of engineers and graduate students in the past few years. The authors would like to thank all the partners and contributors.

REFERENCES

[1] T. Tajima and J. M. Dawson, "Laser Electron Accelerator", *Phys. Rev. Lett.*, vol. 43, pp. 267-270, 1979.

[2] A. Pukhov, "Three-dimensional simulations of ion acceleration from a foil irradiated by a short-pulse laser", *Phys. Rev. Lett.*, vol. 86, pp. 3562-3565, 2001.

[3] S. Wilks, *et al.*, "Energetic proton generation in ultraintense laser–solid interactions", *Phys. Plasmas*, vol. 8, pp. 542-549, 2001.

[4] I. J. Kim, *et al.*, "Transition of proton energy scaling using an ultrathin target irradiated by linearly polarized femtosecond laser pulses", *Phys. Rev. Lett.*, vol. 111, p. 165003, 2013.

[5] T. Esirkepov, *et al.*, "Highly efficient relativistic-ion generation in the laser-piston regime", *Phys. Rev. Lett.*, vol. 92, p. 175003, 2004.

[6] X. Yan *et al.*, "Generating high-current monoenergetic proton beams by a circularly polarized laser pulse in the phase-stable acceleration regime", *Phys. Rev. Lett.*, vol. 100, p. 135003, 2008.

[7] I. J. Kim *et al.*, "Radiation pressure acceleration of protons to 93 MeV with circularly polarized petawatt laser pulses", *Phys. Plasmas*, vol. 23, p. 070701, 2016.

[8] L. Silva, *et al.*, "Proton shock acceleration in laser-plasma interactions", *Phys. Rev. Lett.*, vol. 92, p. 015002, 2004.

[9] H. Habara, *et al.*, "Ion acceleration from the shock front induced by hole boring in ultraintense laser-plasma interactions", *Phys. Rev. E.*, vol. 70, p. 046414, 2004.

[10] L. Yin, *et al.*, "Three-dimensional dynamics of breakout afterburner ion acceleration using high-contrast short-pulse laser and nanoscale targets", *Phys. Rev. Lett.*, vol. 107, p. 045003, 2011.

[11] P. R. Bolton, "The integrated laser-driven ion accelerator system and the laser-driven ion beam radiotherapy challenge", *Nucl. Instr. Meth.*, vol. 809, pp. 149-155, 2016.

[12] M. Borghesi *et al.*, "Proton imaging detection of transient electromagnetic fields in laser-plasma interactions", *Rev. Sci. Instrum.*, vol. 74, pp. 1688-1693, 2003.

[13] L. Romagnani *et al.*, "Dynamics of electric fields driving the laser acceleration of multi-MeV protons", *Phys. Rev. Lett.*, vol. 95, p. 195001, 2005.

[14] S. Busold *et al.*, "Towards highest peak intensities for ultrashort MeV-range ion bunches", *Sci. Rep.*, vol. 5, p. 12459, 2015.

[15] U. Linz and J. Alonso, "What will it take for laser driven proton accelerators to be applied to tumor therapy", *Phys. Rev. ST Accel. Beams*, vol. 10, p. 094801, 2007.

[16] T. Tajima, H. Dietrich and X. Yan. "Laser acceleration of ions for radiation therapy", *Reviews of Accelerator Science and Technology*, pp. 201-228, 2009.

[17] S. D. Kraft *et al.*, "Dose-dependent biological damage of tumour cells by laser-accelerated proton beams", *New J. Phys.*, vol. 12, p. 085003, 2010.

[18] P. K. Singh *et al.*, "A diagnostic for micrometer sensitive positioning of solid targets in intense laser-matter interaction", *Nucl. Instr. Meth.*, vol. 829, pp. 363-366, 2016.

[19] Y. Gao *et al.*, "An automated, 1 Hz nano-target positioning system for intense laser plasma experiments", submitted for publication.

[20] Q. Liao *et al.*, "Recent progress of proton acceleration at Peking University." in *Proc. IPAC'16*, Busan, Korea, May 2016, paper TUPMY018, pp. 1588-1591.

[21] R. Li *et al.*, "Compact laser plasma accelerator at Peking University." in *Proc. IPAC'16*, Busan, Korea, May 2016, paper WEPMY011, pp. 2569-2571.

[22] K. L. Lancaster *et al.*, "Temperature profiles derived from transverse optical shadowgraphy in ultraintense laser plasma interactions at $6 \times 10^{20} \text{ W cm}^{-2}$ ", *Phys. Plasmas*, vol. 16, p. 056707, 2009.

[23] N. Booth, *et al.*, "Target positioning and alignment on the Astra-Gemini facility." in *Proc. SPIE*, San Diego, United States, October 2013, p. 885001.